Journal of Hydrology (N.Z.) Vol. 28, No. 1, 1989

RECONSTRUCTION OF THE RECENT FLOW HISTORY OF A BRAIDED GRAVEL RIVER

Trevor B. Hoey

Department of Geography, University of Canterbury, Christchurch 1, New Zealand

ABSTRACT

Critical tractive stress is used to reconstruct recent flows in the Kowai River, a braided gravel-bed river near Springfield, New Zealand. The method is sensitive to selection of the dimensionless shear stress at which entrainment is presumed to occur, and to variation in the measured parameters of slope and particle size. The importance of cluster bedforms in the Kowai leads to the choice of 0.06 for the critical dimensionless shear stress. Flood magnitudes that correspond well with the two year flood of the river were obtained using a technique of reconstructing the river bed at the time of deposition of the various bar units. Combination of discharge estimates with geomorphic evidence permits interpretation of current river bed morphology in terms of three recent flow events.

INTRODUCTION

Coarse gravel deposits commonly have been used in palaeohydrologic reconstruction in recent years (Baker, 1974). The numerous methods used fall into two categories — hydraulic and geomorphic (Maizels, 1983). The hydraulic approach aims to reconstruct local, instantaneous flow conditions responsible for the emplacement of a single deposit. Measureable characteristics of gravel deposits (usually particle size, sometimes bedforms e.g. Koster, 1978), are related to the flow conditions at the time of deposition by means of empirical relationships obtained from field and/or laboratory work. Contrastingly, the geomorphic approach uses relationships between gross channel characteristics and equilibrium flow regimes. Such methods are best suited to the analysis of long-term variations in discharge, and include the qualitative analysis of Schumm (1969), and regime, discharge-form, discharge-area, and channel pattern equations (Maizels, 1983; Starkel and Thornes, 1981). These approaches reconstruct flows using widely-exposed sedimentary units.

This discussion is concerned with the reconstruction of recent flows in a gravel-bed river, using the hydraulic approach. The transfer of relationships from engineering hydraulics to geomorphological study (Baker, 1974) is not always readily achieved, given the range of assumptions made in engineering studies that may be violated under natural conditions. The hydraulic approach must therefore be used cautiously, ensuring that the methods used are applicable to the conditions under investigation.

The subsequent discussion uses critical tractive stress to reconstruct flow. The technique has general applicability to braided rivers. This method, and its sensitivity to changes in controlling assumptions, are evaluated using data for

the Kowai River, near Springfield, New Zealand. Extension of the results presented herein to other rivers may require variation in some of the assumptions made.

CRITICAL TRACTIVE STRESS THEORY AS A BASIS FOR PALAEOHYDROLOGY

Palaeohydrologic reconstruction involves estimation of a particular flow discharge using a range of methods including critical velocity for entrainment of given particle sizes (using the Hjulstrom curve, or variations thereof; Novak, 1973), transporting capacity of the flow (Baker, 1974), empirical shear stress — particle size relationships (Baker and Ritter, 1974), and critical tractive stress for entrainment of particles of a given size. The last approach gives the most satisfactory results (Maizels, 1983).

In critical tractive stress theory the largest particles present in a deposit (the definition of 'largest' is considered below) are assumed to be the largest that the flow was competent to entrain. It is further assumed that sediment of larger sizes was available, and that all the sediment was fluvially entrained from a river bed. Mean bed shear stress, τ_o, is defined for steady flow as;

$$\tau_o = \gamma_f R S_e \tag{1}$$

where γ_f = unit weight of fluid, R = hydraulic radius, and S_e = the energy slope of the flow. Shields (1936) adapted this relationship for sediment entrainment by the definition of two dimensionless ratios:

$$\theta = \tau_o/(\gamma_s - \gamma_f)\, d \tag{2}$$

$$\text{Rep} = u^* d/\upsilon \tag{3}$$

where θ = dimensionless shear stress, γ_s = the unit weight of sediment, d = particle size, Rep = particle Reynolds number, u* = shear velocity, and υ = kinematic viscosity.

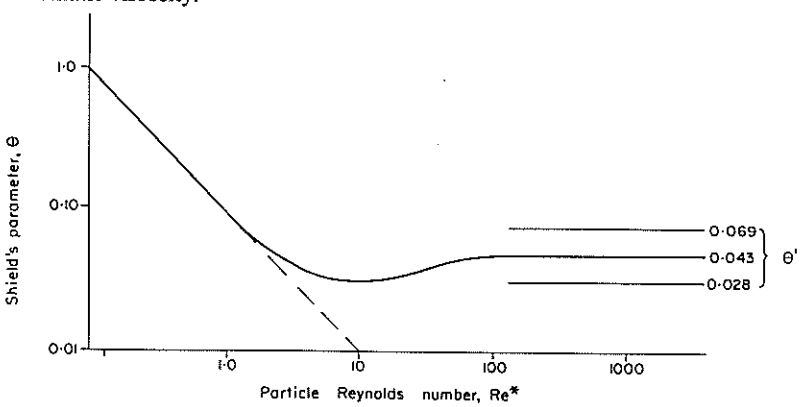

FIG. 1—The Shields entrainment function, showing the envelope of published data for the value of θ when Rep > 100. (after Yalin and Karahan, 1979)

Shields' plot of θ vs. Rep has been widely reproduced with additional data. Figure 1 (after Yalin and Karahan, 1979) is a recent version, based on data for a range of sediment densities and grain sizes. Figure 1 shows that, for values of Rep greater than about 100, the Shields entrainment function, θ, takes on a constant value, as viscous effects are insignificant in fully turbulent flow. In gravel streams, with median grain diameter, d_{50}, of the order of 16–64 mm, a constant value of θ can be assumed. Combining equations (1) and (2) produces;

$$\theta = \gamma_f R S_e / (\gamma_s - \gamma_f)\, d$$

Mean depth, $\bar{h}$, is usually substituted for hydraulic radius, R, provided that the width-depth ratio ($w/\bar{h}$) of the flow exceeds about 15 (Hey, 1979). This implies an error in the $R = \bar{h}$ assumption of about 10% for rectangular or trapezoidal (45° banks) channels. Reduction of the error to 5% requires a width-depth ratio of 38 and 34 for rectangular and trapezoidal channels, respectively. For wide braided rivers at sediment transporting flows, a $w/\bar{h} > 38$ is commonly found (a range of 40.4 to 1070 for $w/\bar{h}$ is found in the studies of Carson (1984) and Church (1972, 1983)). The $R = \bar{h}$ substitution is made here, as is bed slope for energy slope (Maizels, 1983), since bedslope is the only regularly available measure of slope for palaeohydrologic work. It is also assumed that mean bed shear stress is developed entirely as grain stress.

Using these substitutions, and taking $(\gamma_f)/(\gamma_s - \gamma_f)$ as $1/1.65$, gives;

$$\theta = hS/1.65d \qquad (4)$$

Ignoring for the moment the question of the appropriate value of θ to use, and taking Shields' value of 0.06 for incipient motion, (4) becomes;

$$h = 0.099\, d/S \qquad (4a)$$

To calculate other flow parameters an estimate of roughness is required. Alternative means of obtaining these were described by Maizels (1983), and a selection is discussed below. Use of a roughness estimate in combination with flow depth allows velocity estimation and, where flow width is known, discharge, Q, follows from the continuity equation $Q = w.\, \bar{h}.\, \bar{u}$ (where $\bar{u}$ = mean velocity).

SOURCES OF UNCERTAINTY IN USING CRITICAL TRACTIVE STRESS THEORY IN BRAIDED RIVERS

Variations in the derivation of equation (4a) and the assumptions underlying the method were discussed by Maizels (1983), some are of specific relevance to this study.

Possible entrainment mechanisms

The critical tractive stress approach assumes that particle entrainment results from fluid shear on bed particles. Lift forces are implicitly included within the derivation of the Shields parameter (Graf, 1971). Entrainment can occur at lower shear velocities than are theoretically predicted (Andrews, 1983; Baker, 1974) during bank or bar face collapse, where the channel bed or walls slope appreciably

in a cross-channel direction, or where slope material is directly input into channels.

The relationship between flow shear stress and deposition is less well understood than that for entrainment. Using Hjulstrom's (1935) data, the flow velocity at cessation of transport as a percentage of that at entrainment is 48% for 4 mm diameter particles, rising to 78% for 64 mm material. Reid and Frostick (1984) reported ratios between mean bed shear stress at initial and final bedload motion in a gravel-bed (d_{50} = 16 mm) stream ranging between 1.2 and 6.2. Allowing for this difference in conditions at entrainment and deposition is difficult given the paucity of data for the latter case. As most deposition occurs on the falling stage of a flood, reconstructions based on deposits are unlikely to estimate peak flood magnitudes. For these reasons an approach based on entrainment conditions is pursued herein, with the limitations that this imposes being acknowledged.

Value of θ for Rep $>$ 100

The value of θ for Rep $>$ 100 (the constant portion of Figure 1) is uncertain, due to the wide scatter of data from entrainment from plane bed conditions, and to the variety of results from studies of natural conditions in gravel rivers. Shields' (1936) data suggested $\theta' = 0.06$ (where θ' is defined as the value of θ for Rep $>$ 100), but this is no longer considered reliable in all cases (Andrews, 1983; Reid and Frostick, 1984; Yalin and Karahan, 1979). Subsequent data (Yalin and Karahan, 1979; Figures 1 and 5) have suggested $\theta' = 0.047$ (Zeller, 1963, quoted by Graf, 1971), 0.05 (Yalin, 1972) and 0.043 (Yalin and Karahan, 1979). However, only one of the data sets reviewed in this last study was from gravel bed conditions. The use of different materials, and hence grain geometries, in their data could account for the variation of θ'. As Yalin (1972) suggested, a family of Shields curves with each representing a different material geometry would be useful. Additional variability is due to different definitions of the "critical" condition by different workers, and the statistical nature of the entrainment process (the Shields curve shows average values of shear stress (Graf, 1971)).

Observations of θ' lie in the range $0.028 < \theta' < 0.069$, with a mean of $\theta' = 0.043$ (+/– 0.007) (calculated from data reported by Yalin and Karahan, 1979, Figure 5) which can be rounded off to 0.04.

The relevance of this average to field conditions is not obvious, given the effects of particle interaction (Einstein, 1950; Brayshaw, 1985). Fenton and Abbott (1977) suggested that the Shields diagram becomes less relevant as bed geometry departs from the plane bed conditions used in its construction. Their data suggested $\theta' = 0.03$ for initial displacement of co-planar beds, and $\theta' = 0.01$ for erosion of coarse natural sediments. This last value may be too low for natural conditions, given its derivation from data for spherical grains, resting on top of a carpet of hemispheres. The relative protrustion effect investigated by Fenton and Abbott (1977) may be outweighed by the effects of particle interlocking and hiding (Brayshaw, Frostick and Reid, 1983; Reid and Frostick, 1984). Reid and Frostick's data plot close to, but generally above, the Shields curve, and for d_{50} size they found that $0.075 < \theta' < 0.5$, with $0.025 < \theta' < 0.1$ for d_{90} material. Thus for d_{90}, an average value close to $\theta' = 0.06$ is suggested, although this coincidence is probably fortuitous given the opposing effects of particle interaction and relative protrusion. Balancing these two effects is a source of difficulty in selection of a value of θ'. Fenton and Abbott's data are useful, but lack field calibration, so it is not clear how they apply to field conditions. The role of particle clusters in Turkey Brook (Reid and Frostick, 1984) may be atypical, although similar

examples are provided by Laronne and Carson (1976), Cheetham (1979), and Brayshaw (1985). Andrews (1983) shows how θ' can be correlated with particle size and the development of armouring and can be predicted from the empirical equation (5).

$$\theta' = 0.0834\ (d_i/d_{50}')^{-0.872}\ (0.3<d_i/d_{50}'<4.2) \quad (5)$$

where d_i = diameter of the ith percentile fraction of surface material, and d_{50}' = the median diameter of the sub-pavement material. Equation (5) suggests that θ' is greater for a given particle if the sub-pavement is larger, than if it is smaller. The shape of the θ' vs d_i curve suggests that the majority of available material sizes are entrained within a narrow range of shear stress, and Andrews suggested $\theta' = 0.02$ for the largest material in naturally sorted riverbeds. d_i/d_{50}' can be taken as a measure of relative protrusion, but (5) fails to account for shape, sorting or particle density (Carson and Griffiths, 1985). This suggests Andrews' data gives shear stresses which are too low for situations where particle interlocking is important.

At present there is no clear way to resolve the question of the relative effects of grain exposure and particle interaction. Church (1978) classified sediments as normally loose (with about 50% of the grains readily available for entrainment), overloose, and underloose. Suggested values of θ' are 0.05, 0.02 and 0.07, respectively (Church, 1978). Recent work suggests a value of close to 0.04 for normally loose beds, and the value of 0.07 for underloose beds is close to the value of 0.06 for a similar condition in Turkey Brook (Reid and Frostick, 1984). The value of 0.02 for overloose beds is the same as that suggested by Andrews (1983); although this bed state is unusual in natural rivers, Andrews' data may have been collected from a situation where the bed was overloose. Where particle interaction is apparent a value of $\theta' = 0.06$ is suggested, with 0.04 in most other cases, unless the bed is clearly underloose when 0.02 is more appropriate.

Definition of material used

The particle size used for roughness estimation is generally derived from surface or bulk samples from a small area of the bed (1 × 1 m is often used) (Mosley and Tindale, 1985). Such samples may be inadequate for estimating the competent particle size, since the largest material moved by a flow may only occupy a small (say 1%) area of the deposit surface, and is unlikely to be represented in a random 1 m × 1 m sample. Competent size has been estimated from the mean of a certain number of the largest clasts in a deposit (Maizels, 1983), which can include a larger area in the sampling procedure. Definition of the competent size needs to be consistent with the choice of θ'. For conditions where particle interaction occurs, a value of $\theta' = 0.06$ is suggested, where the whole bed behaves as if made up of d_{90} size material (Reid and Frostick, 1984). In this case use of d_{90} as the competent size is suggested. This is not the largest material moved by the flow, but is the size for which θ' has been chosen.

Validity of the assumptions of critical tractive stress theory

Maizels (1983) listed these assumptions, two of which are discussed here. Firstly the relevance of equation (1) to turbulent, rapidly varied flow in gravel rivers is uncertain. Cheetham (1979) measured local bed shear stresses up to 10 times those predicted by equation (1), and the distribution of shear stress in natural

channels is non-uniform (Graf, 1971; Bathurst, 1979). For flow reconstruction this variability leads to the statistical problem of the probability of the greatest shear stresses being coincident with the locations of the largest material. Uncertainty introduced as a result of using average values alone, should be noted.

Secondly, suspended sediment concentrations in water flows are important, since Shields' entrainment function is dependent partially on the density contrast between the material being entrained, and the fluid (Equation (2)). In the South Island of New Zealand, for flows five times the mean, fluid densities lie in the range 1.0003 to 1.007 g cm^{-3}, with a mean of 1.002 g cm^{-3} (Thompson and Adams, 1979). The mean value is lower than the 1.005 g cm^{-3} suggested by Koster (1978). The data set includes numerous rivers in locations similar to the study area, so a value of 1.002 g cm^{-3} is used.

Synopsis

There is uncertainty as to what values of parameters should be used, at various stages of flow reconstruction and as to the effects of different sedimentary and flow conditions. At present only order-of-magnitude estimates of discharges are attainable (Church, 1978; Maizels, 1983), although accuracy is greater for the upper range of flow conditions (Church, 1978). Several problems arise with this approach:

(a) Grain size heterogeneity, bed microtopography and hiding effects, combined with flow fluctuations, render the entrainment process probabilistic (Church, 1978; Richards, 1982). Entrainment is not functionally dependent upon mean conditions (Church, 1978), but allowing for this introduces complex statistical problems.

(b) The relationship between flow competence and the largest size of material present in a deposit, is poorly understood.

(c) Reconstructions, although based on deposits, attempt to estimate entrainment conditions. Conditions at entrainment and deposition differ (Hjulstrom, 1935; Reid and Frostick, 1984), but the nature of these differences is poorly understood.

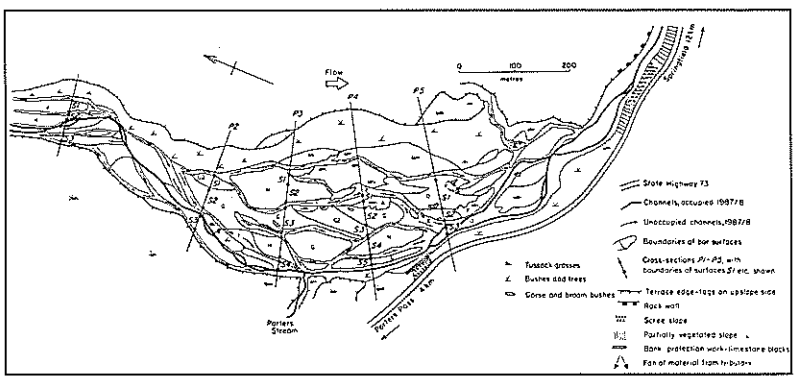

FIG. 2—Morphological map of the study reach, Kowai River. The locations of the five cross-sections used, P1–P5, are shown. S1, S2 etc. refer to bar surfaces for which flow was reconstructed. Bar and channel locations A-O are explained in the text.

These problems can be minimised by consideration of the assumptions involved and by obtaining more than one estimate of flow by independent means, wherever possible.

STUDY SITE AND DATA COLLECTION

Data were collected from a reach of the Kowai River, near Springfield, South Island, New Zealand. Reach slope is 0.023, and two-year flood is about 120 m^3s^{-1}. At all but the lowest flows (< 1 m^3s^{-1}) the river occupies multiple channels in the study reach, and can be classified as braided. Figure 2 shows the location of the five cross-sections used for this analysis. Each section was surveyed and divided into separate bar units.

Large contiguous units were chosen, with measurements made of bed slope, surface particle size in a 1 m × 1 m quadrat, sub-surface particle size (bulk sample),

TABLE 1—Width, slope and grain size of the 18 surfaces used in the palaeoflow analysis.

Surface	Width (m)	Slope	Surface d_{90} (m)	Surface d_{10x} (m)
P1/S1	17.9	0.027	0.118	0.260
P1/S2	11.5	0.030	0.161	0.290
P1/S3	5.3	0.019	0.116	0.270
P2/S1	6.8	0.027	0.054	0.210
P2/S2	27.5	0.025	0.084	0.250
P2/S3	13.1	0.020	0.047	0.140
P3/S1	7.7	0.023	0.051	0.230
P3/S2	14.5	0.037	0.097	0.200
P3/S3	78.7	0.021	0.119	0.260
P3/S4	4.3	0.029	0.115	0.280
P4/S1	12.7	0.025	0.155	0.260
P4/S2	16.2	0.030	0.060	0.210
P4/S3	23.8	0.036	0.054	0.220
P4/S4	22.2	0.021	0.061	0.180
P4/S5	11.1	0.023	0.098	0.180
P5/S1	24.9	0.034	0.095	0.220
P5/S2	22.2	0.035	0.054	0.190
P5/S3	7.9	0.019	0.074	0.160

FIG. 3—Example of the type of particle cluster that occurs widely on the bed of the Kowai in the study reach. Flow was left to right. Stake is 1 m long.

and the size of the 10 largest fluvially transported clasts present. Slope was surveyed along a line approximately 50 m in length, centred on the cross-section of interest, in the direction of maximum slope. Linear regression through the surveyed points provided the slope estimate. These data are shown in Table 1. All measurements were made directly on the cross-section, except for measurements of the largest material present, which were taken over a 10 m wide area, centred on the cross-section.

RESULTS

The five cross-sections provided 18 individual surfaces for analysis. Only maximum flows were of interest so smaller bar surfaces cut into these were discounted.

Evaluation of the critical tractive stress approach

The bed microtopography in the study reach is dominated by cluster bedforms (Figure 3). Morphologically these appear to be intermediate between linear, flow parallel clusters (Brayshaw, 1985) and transverse clast dams (Bluck, 1987), being either wide versions of the former, or narrow ones of the latter. The abundance of such bedforms, suggests use of $\theta' = 0.06$, and hence of surface material d_{90} as the competent particle size, implying that the bed is 'underloose' (Church, 1978). Use of Andrews' (1983) equation (5) to estimate θ' is not feasible, since the value of d_{90}/d_{50}' is in the range $2.6 < d_{90}/d_{50}' < 20.2$ (mean = 9.1), which is generally outside the range 0.3–4.2 for which (5) was developed.

Taking $\theta' = 0.06$, and using surface d_{90} as the competent particle size, the 18 surfaces gave flow depths predicted from equation (4a), h, in the range 0.15 m

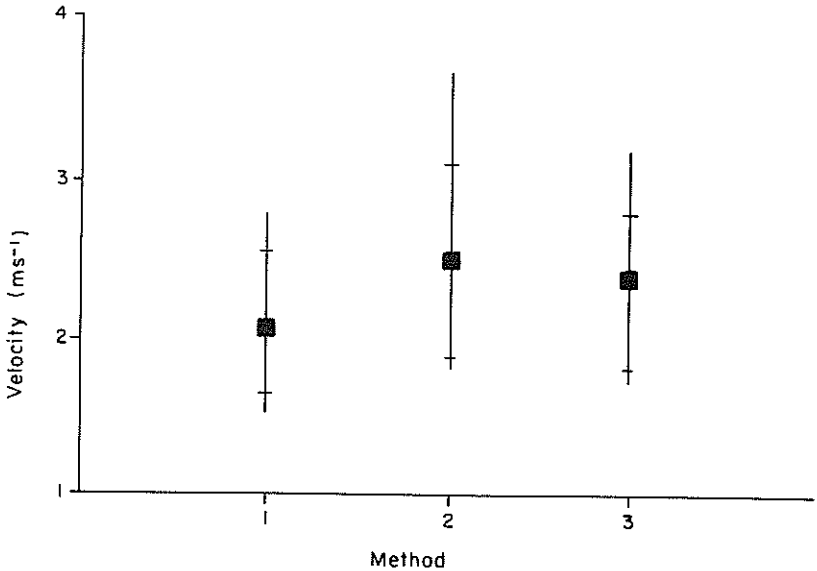

FIG. 4—Velocity estimates using three methods to calculate roughness. Squares show mean values; tick marks at +/− 1 standard deviation; lines show the range of data (n = 18). The methods are; 1. Limerinos-Manning (Equations 6, 6a); 2. Griffiths-Darcy-Weisbach (7, 8a); 3. Bray-Davar-Darcy-Weisbach (8, 8a).

$\leqq h \leqq 0.61$ m ($\bar{h} = 0.35$ m). d_{90} was between 0.047 and 0.161 m, and slopes were in the range, 0.019–0.037. Velocity determination requires the combination of the depth data with a roughness estimator. Maizels (1983) assessed the performance of five roughness estimation methods, concluding that the Limerinos-Manning approach (combining the Manning equation with the work of Limerinos, 1970) is preferable where flow width is uncertain. The Limerinos-Manning method (6), and two others, by Griffiths (1981a) (7), and Bray and Davar (1987) (8), have been compared for the Kowai data (Fig. 4).

The Limerinos (1970) equation is

$$n = 0.113R^{1/6}/[1.16 + 2\text{Log}\,(R/d_{84})] \tag{6}$$

with u determined from the Manning equation,

$$\bar{u} = R^{2/3}\,S^{1/2}/n \tag{6a}$$

Griffiths' (1981) equation is

$$1/\sqrt{f} = 0.760 + 1.98\,\text{Log}\,(R/d_{50}) \tag{7}$$

and Bray and Davar (1987) provided

$$1/\sqrt{f} = 1.9\,(R/d_{84})^{1/4} \tag{8}$$

both of which calculate velocity from

$$\bar{u} = (8\ gRS/f)^{1/2} \quad (8a)$$

In the above, n and f are the Manning and Darcy-Weisbach roughness coefficients, respectively, d_{84} = particle size for which 84% is finer, and g = acceleration due to gravity (9.81 ms^{-2}).

Consistent prediction of the lowest velocity values and the least scatter in the data, justify use of the Limerinos equation herein. The wider scatter in the Darcy-Weisbach-Griffiths (7,8a) and Darcy-Weisbach-Bray-Davar methods could reflect either the greater sensitivity or the lesser reliability of these methods. Palaeoflow reconstruction based on conditions at entrainment estimates the lowest flow conditions of the palaeohydrological methods, flows which are likely to be below flood peak magnitudes. A roughness parameter that gives the lowest estimated velocities is preferred to maintain consistency in under-estimating likely flood maxima. At greater flows resistance tends to be reduced (Parker and Peterson, 1980; Griffiths, 1981a) and a different predictor of velocity may be required.

The three critical input variables for palaeoflow analysis are bed slope, material size, and Shields' parameter θ'. Combining equations (4), (6) and (6a), with the continuity equation (9), gives (10) and (11):

$$q = \bar{h}.\ \bar{u} \quad (9)$$

$$\bar{u} = 11.37\ d_{90}^{\ 1/2} \theta'^{1/2} [1.16 + 2\mathrm{Log}\ (2.19\ \theta'/S)] \quad (10)$$

$$q = 18.76\ d_{90}^{\ 3/2}\ \theta'^{3/2}\ S^{-1}\ [1.16 + 2\mathrm{Log}\ (2.19\ \theta'/S)] \quad (11)$$

where q = discharge/unit width (m^2s^{-1}). In (10) and (11) d_{90}/d_{84} is taken as 1.33 (+/– 0.10), the mean value from the 18 Kowai samples. A sensitivity analysis, using the geometric mean values of d_{90} and S from the Kowai data, and θ' = 0.06 as base values, is shown in Figure 5, using the range of the Kowai data for slope and particle size, and the range suggested from previous studies for θ'. The sensitivity to changes in the controlling variables is indicated by the gradients of the curves (this is only an indication since equation (10) is empirical and not a structural relation). For palaeovelocity, the most sensitive variable is θ', followed by d_{90} and slope. An increase in slope of 0.005 (22% from the base value) produces a 6% decrease in estimated velocity. Similarly, a 20% rise in d_{90} leads to a 10% increase in velocity, and a 0.01 increase in θ' gives a 14% increase in estimated velocity. Slope and particle size are both affected by sampling variability in the field, and 20% errors in their estimation are not unreasonable (Kumar and Devi, 1981; Mosley and Tindale, 1985). Incorrect estimates of θ' by more than 0.01 are possible, as the wide range of estimates in the literature shows; difficulty with the estimation of this parameter is responsible for much of the uncertainty in the palaevelocity determinations.

When unit discharge, q, is considered, a different picture emerges (Equation (11), Figure 5b). For 20%, 20% and 0.01 increases in slope, particle size and θ' respectively, unit discharge estimates change by –27%, +31% and +32%. Except at low slopes (< 0.02) the sensitivity of unit discharge to changes in the three

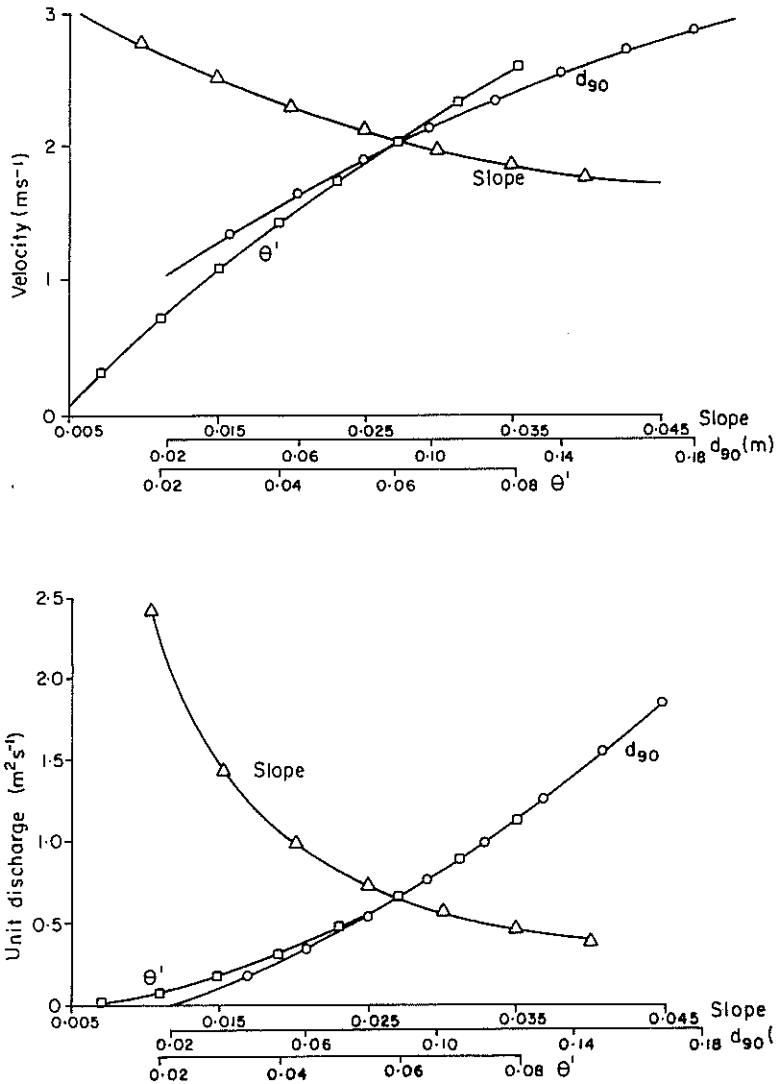

FIG. 5—Sensitivity of predicted velocity and unit discharge to changes in input variables. The base values are S = 0.026; d_{90} = 0.083 m; θ' = 0.06. Equation (10) was used for (a) and equation (11) for (b).

(a) $\bar{u} = 0.80\ [1.16 + 2\text{Log}\ (0.13/S)]$; $\bar{u} = 7.15\ (d_{90})^{0.5}$; $\bar{u} = 3.28\ \theta'^{0.5}\ [1.16 + 2\text{Log}\ (84.23\ \theta')]$.

(b) $q = 0.007\ [1.16 + 2\text{Log}\ (0.13/S)]/S$; $q = 27.22\ (d_{90})^{1.5}$; $q = 17.25\ \theta'^{1.5}\ [1.16 + 2\text{Log}\ (84.23\ \theta')]$.

controlling variables is similar. For accurate palaeodischarge estimation, each of these three variables is equally important.

Bed material size and slope measurement are subject to both random and systematic errors. The random errors, which affect relative flow magnitudes, can be reduced to some extent by consistent measurement procedures. Flow magnitudes estimated using d_{90} and d_{10x} (average size of the 10 largest clasts on a surface) in equation (4a) are correlated at the 0.005 significance level. Relative flow magnitudes are thus independent of the particle size measure chosen. Specification of absolute flow magnitudes is made difficult by the presence of the systematic errors. The cumulative effects of errors in slope, particle size and θ' in equations (10) and (11) are potentially great. In the extreme case where errors do not cancel out at all, a 20% increase in particle size, 20% decrease in slope, and 0.01 increase in θ' relative to the base values above, produce changes of + 35% in palaeovelocity and +148% in unit palaeodischarge. If θ' is unaltered, the changes are +20% and +87% respectively. Not enought is known about the sampling distribution of either slope or particle size, or about the distribution of θ', to determine the most probable error. Assuming that the same value of θ' is relevant for all the 18 Kowai surfaces analysed, any errors due to mis-specification of θ' will be approximately equivalent in percentage terms, so that relative flow magnitudes can be reliably assessed. Consistency in the measurement procedures used for slope and particle size should reduce systematic errors in

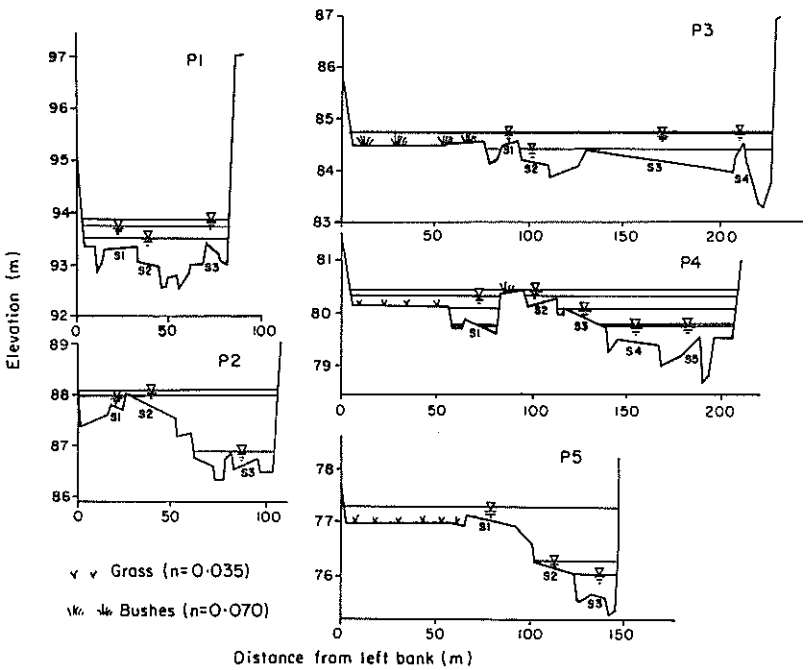

FIG. 6—Cross-sections used in palaeoflow analysis. Vertical exaggeration is x 28. See Figure 2 for locations. Water surfaces associated with the bar surfaces are shown. The water surface symbol is drawn directly above its associated bar surface.

these variables. Likely errors of +/- 10% and +/- 20% in velocity and unit discharge are assumed in consideration of relative flow magnitudes, although the choice of these values is somewhat arbitrary.

Palaeodischarge analysis for the Kowai River

The five cross-sections used for palaeodischarge analysis are shown in Figure 6. The water depth associated with each of the sedimentary surfaces indicated was calculated using equation (4a), the slope of each surface and d_{90} of the surface material. Two methods of discharge reconstruction were then used for each cross-section:

(a) the surveyed cross-section was used as the cross-section at the time of formation of the surface; and

(b) the elevation of the surface was used as a minimum bed level at the time of surface formation (see cross-section P1, Figure 7).

Method (a) gives larger discharge estimates than method (b), since it deals with a larger cross-sectional area of flow. The roughness values (n) given by equation (6) were increased by a factor of 1.37, to allow for the effect of bar roughness. Equation (6) accounts for roughness due to grain-fluid interaction (Robert, 1988), but larger scale form (bar) roughness is omitted. Bar roughness is applicable only when discharge through a whole cross-section is being calculated, since it does not influence roughness over individual point locations. Estimates of the effect of bar roughness range from <10% of resistance at high flow (Parker and Peterson, 1980), to 50–60% (Prestergaard, 1983). A comparison of the methods used by Parker and Peterson, and Prestergaard, is given in Table 2, which includes two New Zealand data sets. The data in Table 2 suggest that bar roughness accounts for more than the 10% suggested by Parker and Peterson.

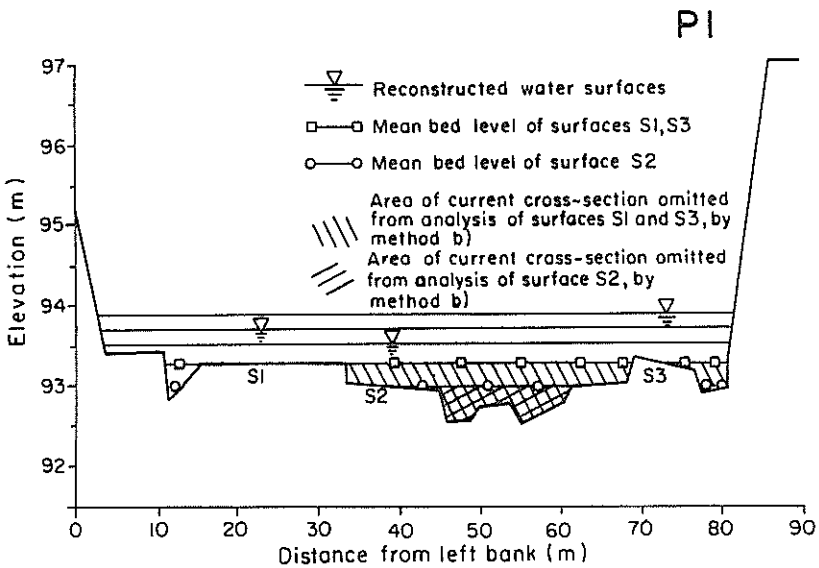

FIG. 7—Example of the procedure used to reconstruct the bed surface at the time of the flow events. See text for explanation of the reconstruction method (b).

TABLE 2—Grain slope as a percentage of total slope

River type	Sample Size	Method 1 Mean (%)	S.D. (%)	Range (%)	Method 2 Mean (%)	S.D. (%)	Range (%)	Data Source
Meandering	6	31	11	13–41	45	17	18–68	Carson (1984)
Braided	4	32	7	22–38	47	11	32–57	Carson (1984)
Divided	6	37	11	25–47	66	20	44–89	Prestergaard (1983)
Straight	6	28	18	7–66	49	32	11–100	Prestergaard (1983)
Stable bed	84	59	24	11–100	81	22	19–100	Griffiths (1981a)
Mobile bed	52	53	17	19–84	73	22	30–100	Griffiths (1981a)

Method 1 follows Prestergaard (1983), using d_{84} as the roughness height

Method 2 follows Parker and Peterson (1980), using 2 d_{90} as the roughness height

S.D. is standard deviation

Considerable scatter in the data is due to measurement errors and differences in measurement procedures. Bankfull conditions are improbable in the Kowai River due to its partial confinement by fluvioglacial terraces, so the mobile bed data of Griffiths (1981a) are the most applicable. This data set suggests a grain slope : channel slope ratio of about 0.53 using Prestergaard's (1983) method, which was selected as it suggests that grain slope is a lower percentage of total slope than does the Parker and Peterson (1983) method. Thus estimates obtained for velocity are lower than with the latter method. This correction involves multiplication of the roughness value, "n", by 1.37.

Methods (a) and (b) can be evaluated by comparing their predicted palaeodischarges with the mean annual flood of 120 m^3s^{-1} for the Kowai at Limeworks Bridge estimated by Blakely, Ackroyd and Marden (1981). This flow may be slightly lower in the study reach due to tributary inputs above Limeworks Bridge, but provides a useful order of magnitude estimate of expected flows. A large flow event occurred in this river in March 1986, and between January and June 1987 another event caused the main low flow channel to switch from being close to the left bank to the right bank in this reach. One or more other events are thought to have occured in the latter part of 1986. It appears from the frequency distribution of the 18 reconstructed flows that method (a) overpredicts discharge (Figure 8). 11 of the 18 discharges calculated by this method exceed 120 m^3s^{-1}, with a maximum of 467 m^3s^{-1}. This is equivalent to 11.9 m^3s^{-1}/km^2 of catchment, which is considerably above discharge/catchment area figures for South Island catchments in a 10-year flood (Q_{10}; data from Griffiths, 1981b). For Canterbury and Marlborough rivers Q_{10}/Basin area is 0.95 +/– 0.41 m^3s^{-1} km^{-2}, but higher values would be expected from smaller catchments such as the Kowai (39.1 km^2). The maximum flow predicted by method (b) is 178 m^3s^{-1}, representing 4.6 m^3s^{-1} km^{-2}, which is not unreasonable.

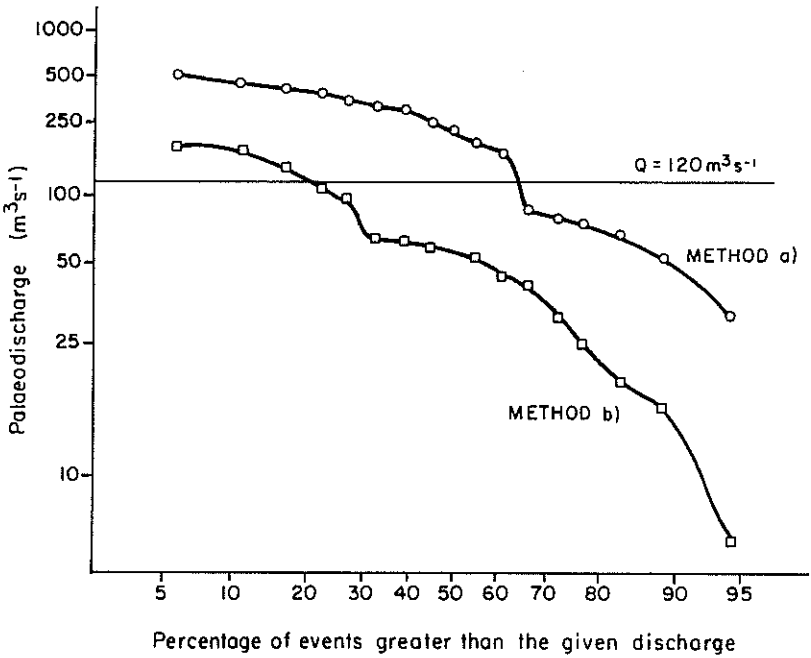

FIG. 8—Log-probability plot of the discharges calculated from the 18 bar surfaces in the Kowai River. See text for explanation of methods (a) and (b). 120 m^3s^{-1} is the approximate two year flood in the Kowai.

The frequency distribution of calculated discharges using method (b) shows a clear discontinuity at about 90 m^3s^{-1} (Fig. 8), which also shows on Figure 9, where the 18 discharges are plotted in rank order, with +/- 20% error bars shown. This discontinuity is taken as one of two primary discontinuities, breaks in the discharge series with zero overlap between the error bar of one discharge value and that of the next one in the series. Secondary discontinuities (Fig. 9) have overlaps in the error bars, but neither error bar overlaps the value of the predicted discharge itself. Two primary, two secondary, and one possible secondary discontinuity in the series are identified.

Comparison of the palaeodischarge analysis with geomorphological evidence

The five cross-sections used are located relative to the main elements of the river bed morphology in Figure 2. Event 3c (Fig. 9) contains two surfaces: cross-section 4, surface 1 (P4/S1), and cross-section 3, surface 3 (P3/S3). P4/S1 is a small surface, attached to the left bank of a stable vegetated island (A on Figure 2), and appears to be a remnant surface from an earlier event which cut into this island. P4/S1 may not be a consequence of one of the recent events outlined above. P3/S4, which is the sole surface associated with event 3b, is atypical in that it is located in the lee of a very stable and persistent vegetated island (present on 1974 aerial photographs). Hydraulically this is an unusual location, and this may have influenced the estimated discharge. Alternatively, this surface may be associated with a large event some time

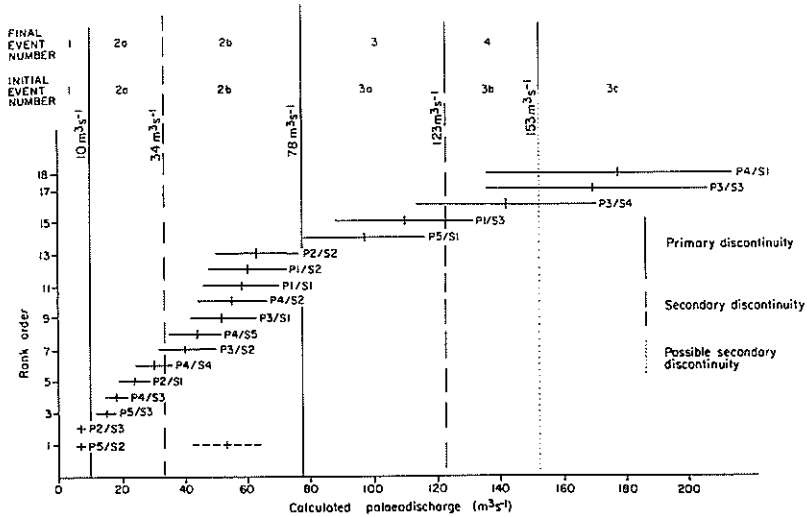

FIG. 9—Discharge series for the 18 calculated palaeodischarges. Predicted values are shown +/– 20%. P5/S3 refers to cross-section 5, surface 3 etc. See text for explanation of event numbers and primary and secondary discontinuities. The horizontal dashed line is discharge calculated by method (a) for P5/S2.

previously (re-numbered as event 4). Event 3a (P1/S3 and P5/S1) may be the March 1986 event, or another later in the same year. P5/S1 is markedly higher than the rest of cross-section 5 (Fig. 6), with both P5/S2 and P5/S3 appearing to be cut into it, suggesting its earlier deposition. The main channel was formerly in channel C, and is presumed to have flowed out over surface D, prior to the development of the more recently occupied channel E (Fig. 2). The persistence of island fragments F, which is inferred from the mature gorse and broom growing on them, suggests that flow over D was diffuse rathern than channelised. P1/S3, which is also within event 3a, is considerably dissected. Although it lies below P1/S1, its location on the inside of a bedrock and terrace-controlled bend could have preserved it during the event that formed P1/S1.

On the basis of the above evidence, a single event 3 is postulated, with the possibility of a much earlier event (event 4 in the final event order; Figure 9) which formed P3/S4. Based on P5/S1 and P1/S3, the magnitude of this flow is taken as 104 +/– 26 m^3s^{-1}.

Events 2a and 2b produced a large number of surfaces, most of which are in the areas G and M on Figure 2. P3/S3 is anomalous in this, as it plots in event 3c, but appears to be part of morphological unit G. Additional survey data for cross-section P3 (Fig. 6) shows that surface H is lower than G, and that the boundary between the two should be stepped. Identification of P3/S3 as a single surface may be in error, and H could have been modified when channel I was occupied. In addition, P3/S3 has a low slope (0.021), which may be an underestimate of the true value. Since the morphological evidence suggests that the palaeodischarge estimate for P3/S3 is in error, it is discounted from further consideration. Event 2b (presumably March 1987) formed the extensive surface G, in addition to J, K, L and M. Surface G was then locally eroded

TABLE 3—Suggested chronology for formation of riverbed surfaces

Event	Surfaces formed in event	Approximate discharge (m^3s^{-1})	Possible time of occurrence	Water surface slope
1	P2/S3	7+/-1.5	July–Sept. 1987	N.A.
2a	P2/S1, P4/S3 P4/S4, P5/S3	22+/-12	March 1987 — falling stage	0.031
2b	P1/S1, P1/S2, P2/S2 P3/S1, P3/S2, P4/S2, P4/S5, (P5/S2)	55+/-23	March 1987 — peak flow	0.027
3	P1/S3, P5/S1	104+/-26	March 1986 (or later 1986) — peak flow	0.026
4?	P3/S4	142+/-28	Pre-March 1986	N.A.

N.A. — not available

on the falling stage (event 2a, surface G2) as flow became more confined to channel C and the main right bank channel. P3/S2 was cut into P3/S1 in either 2a or 2b, but P3/S1 escaped further erosion due to its greater elevation than P3/S3. Surface L appears now as a channel levee deposit, but may once have been more extensive on its left bank side. Surfaces N and G2 were probably formed contemporaneously, and N may have developed after erosion of a more extensive surface L. As stage fell, surface O was also deposited, obliterating event 2b deposits in this area. P1/S1 and P1/S2 appear to have survived the incision in event 2a, possibly due to bedrock constraints on the channel encouraging the development of a deeper, incised channel at cross-section P1.

Only surfaces P2/S3 and P5/S2, both of which fall into event 1, are unaccounted for. P5/S2 is chaotically dissected and could be a late event 2a remnant. It has a predicted water depth of only 0.14 m, and it is unlikely that the bed level was entirely at or above the level of P5/S2 (Fig. 6). The discharge associated with this surface may therefore be underestimated, and morphologically it appears to fit into event 2a or 2b. Using method (a) to re-estimate the flow associated with P5/S2 gives 53 m^3s^{-1}, which would locate it in event 2b. P2/S3 is likely to be due to a smaller, more recent event, being adjacent to the main channel.

Summary

A summary of the flow events considered responsible for the present bed morphology is given in Table 3, where the events are given the 'Final event numbers' suggested on Figure 9. Of the 18 surfaces, only P4/S1 and P3/S3 have not been used in the Table, for reasons outlined above. Given the uncertainty about event 4, the 3 event structure suggested on the basis of the discharge series alone has been preserved, with the three stages of event 3 being combined into a single event. The three event interpretation is supported by the water surface elevations predicted by the initial critical tractive stress calculations

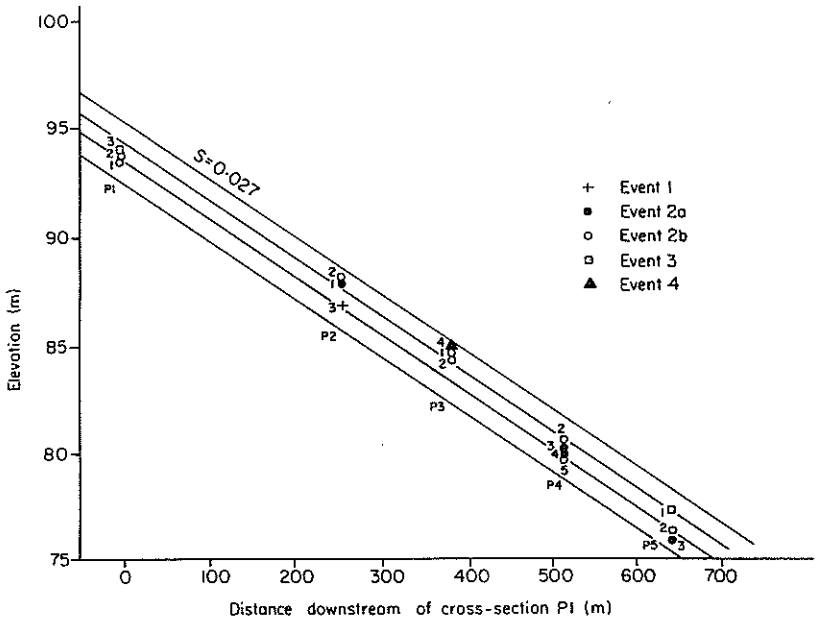

FIG. 10—Water surface elevations calculated for different bar surfaces. See Table 3 for an explanation of events 1–4. Regression lines through both bar and water surfaces have slope, S = 0.027.

(Fig. 10). Without exception, event 3 plots above events 2a and 2b. Event 2b plots above 2a, except for P4/S5, which is unusual in being adjacent to the main channel. Water surface slopes calculated from this data are in Table 3.

CONCLUSIONS

The critical tractive stress approach is a well established basis for palaeoflow reconstruction. The details of its use need to be considered carefully for the particular conditions under investigation. Selection of a roughness estimator appears to be relatively unimportant; this study confirms Maizels' (1983) conclusion that the Limerinos-Manning approach is the most suitable, even when compared with roughness equations developed from rivers of similar type to the Kowai. Palaeovelocity determination is intrinsically more accurate than palaeodischarge, but consistent measurement procedures are essential if reliable results are to be obtained. For determination of absolute discharge values, selection of an appropriate value of θ' remains critical. Naturally sorted gravel in river beds can have a variety of θ' for entrainment, depending upon bed microtopography. Where particle interaction is significant, the conclusions of Reid and Frostick (1984) justify taking $\theta' = 0.06$, when d_{90} is taken as the competent size fraction. Equally useful results may be obtained by use of a lower value of θ', in conjunction with a larger competent size, such as d_{10x}. Appropriate values of θ' may be obtained from equations such as that of Andrews (1983),

derived from different conditions. For determination of absolute discharges, sources of uncertainty in the results from the critical tractive stress approach are (a) measurement error in slope, particle size and cross-section surveys; (b) selection of a θ'–d_x pair; (c) estimation of suspended sediment concentration; (d) reliability of roughness determination; (e) accuracy of estimates of the effect of bar roughness; (f) applicability of shear stress equations to turbulent conditions; and (g) accuracy of bed surface reconstructions.

The absolute discharge values reported must be treated with caution, although they are reasonably consistent with the only flow estimate available for the Kowai by independent means, and produce reasonable discharge/catchment area figures. The values are dependent upon the validity of the bed reconstruction (method (b)) of flow area estimation. Method (a) severely overestimated likely discharges, suggesting that it is important to note the degree of post-flood modification of river bed deposits in calculations of palaeodischarge. Relative discharge estimates are more reliable than the absolute values, in conjunction with geomorphological evidence. Combined, these two sources of information provide a detailed picture of the evolution of the bed of the Kowai over a short time scale. Neither data set alone is able to achieve the same completeness of explanation. The technique can be of considerable use in the investigation of recent river flow history.

ACKNOWLEDGEMENTS

This work was funded in part by a Research Grant from the North Canterbury Catchment Board to Dr J. B. Hockey. Ray Begg and Vanessa Brazier helped with data collection, and Alistair Dyer drew the figures. Burn Hockey commented on an earlier draft of the manuscript, and the comments of two anonymous referees were extremely valuable.

REFERENCES

Andrews, E. D. 1983; Entrainment of gravel from naturally sorted riverbed material. *Geological Society of America Bulletin 94:* 1225–31.

Baker, V. R. 1974: Palaeohydraulic interpretation of Quaternary alluvium near Golden, Colorado. *Quarternary Research 4:* 94–112.

Baker, V. R.; Ritter, D. F. 1975: Competence of rivers to transport coarse bedload material. *Geological Society of America Bulletin 86:* 975–8.

Bathurst, J. C. 1979: Distribution of boundary shear stress in rivers. *In* Rhodes, D. D. and Williams, G. P. (eds): *Adjustments of the Fluvial System.* Kendall Hunt. Dubuque, Iowa: 95–116.

Blakely, R. J,; Ackroyd, P.; Marden, M. 1981: *High Country River Processes.* Tussock Grasslands and Mountain Lands Institute, Lincoln College. Special Publication 22, 94 pp.

Bluck, B. J. 1987: Bed forms and clast size changes in gravel-bed rivers. *In* Richards, K. S. (ed): *River Channels: Environment and Process.* Institute of British Geographers Special Publication 18. Blackwell, Oxford, 391 pp: 159–178.

Bray, D. I.; Davar, 1987: Resistance to flow in gravel-bed rivers. *Canadian Journal of Civil Engineering 14:* 77–86.

Brayshaw, A. C. 1985: Bed microtopography and entrainment thresholds in gravel-bed rivers. *Geological Society of America Bulletin 96:* 218–23.

Brayshaw, A. C. Frostick, L. E.; Reid, I. 1983: The hydrodynamics of particle clusters and sediment entrainment in coarse alluvial channels. *Sedimentology 30:* 137–43.
Carson, M. A. 1984: Observations on the meandering-braided transition, the Canterbury Plains, New Zealand. *New Zealand Geographer 40:* 12–19, 89–99.
Carson, M. A.; Griffiths, G. A. 1985: Tractive stress and the onset of bed particle movement in gravel stream channels: different equations for different purposes. *Journal of Hydrology 79:* 375–88.
Cheetham, G. H. 1979: Flow competence in relation to stream channel form and braiding. *Geological Society of America Bulletin 90:* 877–86.
Church, M. 1972: Baffin Island Sandurs: a study of Arctic fluvial processes. *Bulletin of the Geological Survey of Canada 216:* 208 pp.
Church, M. 1978: Palaeohydraulogical reconstructions from a Holocene valley fill. *In* Miall, A. D. (ed) *Fluvial Sedimentology.* Canadian Society of Petroleum Geologists Memoir 5, 859 pp: 743–72.
Church, M. 1983: Patterns of instability in a wandering gravel bed channel. *In* Collinson, J. D. and Lewin, J. (eds): *Modern and Ancient Fluvial Systems.* International Association of Sedimentologists Special Publication 6: 169–80.
Einstein, H. A. 1950: The bedload function for sediment transportation in open channel flows. *Technical Bulletin No. 1026. United States Department of Agriculture:* 70 pp.
Fenton, J. D.; Abbott, J. E. 1977: Initial movement of grains on a stream bed: the effect of relative protrusion. *Proceedings, Royal Society of London Series A, 352A:* 523–37.
Graf, W. H. 1971: *The Hydraulics of Sediment Transport.* McGraw Hill, New York. 574 pp.
Griffiths, G. A. 1981a: Flow resistance in coarse gravel-bed rivers. *Journal of the Hydraulics Division, Proceedings of the American Society of Civil Engineers 107(7):* 899–918.
Griffiths, G. A. 1981b: Some suspended sediment yields for South Island catchments, New Zealand. *Water Resources Bulletin 17:* 662–71.
Hey, R. D. 1979: Flow resistance in gravel-bed rivers. *Journal of the Hydraulics Division, Proceedings of the American Society of Civil Engineers 105(4):* 365–79.
Hjulstrom, F. 1935: Studies in the morphological activities of rivers as illustrated by the river Fyris. *Bulletin of the Geological Institute, University of Uppsala. 25:* 221–528.
Koster, E. H. 1978: Transverse ribs: their characteristics, origin and paleohydraulic significance. *In* Miall, A. D. (ed) *Fluvial Sedimentology.* Canadian Society of Petroleum Geologists Memoir 5, 859 pp: 161–86.
Komar, P. D.; Z. Li 1986: Pivoting analyses of the selective entrainment of sediments by shape and size with application to gravel threshold. *Sedimentology 33:* 425–36.
Kumar, A.; Devi, R. 1981: Discussion of Parker, G. and Peterson, A.W. 1980 *op cit. Journal of the Hydraulics Division, Proceedings of the American Society of Civil Engineers 107(9):* 1115–6.
Laronne, J. B.; Carson, M. A. 1976: Interrelationships between bed morphology and bed material transport for a small gravel-bed channel. *Sedimentology 23:* 67–85.
Limerinos, J. T. 1970: Determination of the Manning coefficient from measured bed roughness in natural channels. *United States Geological Survey Water-Supply Paper 1898B:* 47 pp.
Maizels, J. K. 1983: Palaevelocity and palaeodischarge determination for coarse gravel deposits. *In* Gregory, K. J. (ed): *Background to Palaeohydrology,* John Wiley, Chichester: 101–39.
Mosley, M. P.; Tindale, D. S. 1985: Sediment variability and bed-material sampling in gravel-bed rivers. *Earth Surface Processes and Landforms 10:* 465–82.
Novak, I. D. 1973: Predicting coarse sediment transport: the Hjulstrom curve revisited. *In* Morisawa, M. (ed): *Fluvial Geomorphology.* Allen and Unwin. London: 13–25.
Parker, G.; Peterson A. W. 1980: Bar resistance of gravel-bed streams. *Journal of the Hydraulics Division, Proceedings of the American Society of Civil Engineers 106 (10):* 1559–75.

Powers, M. 1953: A new roundness scale for sedimentary particles. *Journal of Sedimentary Petrology 25:* 297–301.

Prestergaard, K. L. 1983: Bar resistance in gravel bed streams at bankfull stage. *Water Resources Research 19:* 472–6.

Reid, I.; Frostick, L. E. 1984: Particle interaction and its effect on the thresholds of initial and final bedload motion in coarse alluvial channels. *In* Koster, E. H. and Steel, R. J. (eds): *Sedimentology of Gravels and Conglomerates.* Canadian Society of Petroleum Geologists, Memoir 10: 61–8.

Richards, K. S. 1982: *Rivers: form and process in alluvial channels.* Methuen, London. 358 pp.

Robert, A. 1988: Statistical properties of sediment bed profiles in alluvial channels. *Mathematical Geology 20:* 205–25.

Schumm, S. A. 1969: River metamorphosis. *Journal of the Hydraulics Division, Proceedings of the American Society of Civil Engineers 95(1):* 255–73.

Shields, A. 1936: Anwendung der Aehnlichkeitsmechanik und der Turbulenzforschung auf die Geschiebebewegung. *Mitteil. der Preussischen Versuchsanstalt fuer Wasserbau und Schiffbau. Heft 26.* Berlin (Translated by Ott, W. P. and Van Uchelen, J. C.: *Application of similarity principles and turbulence research to bedload movement.* United States Department of Agriculture, Soil Conservation Service, 70pp).

Starkel, L.; Thornes, J. B. 1981: Palaeohydrology of river basins. *British Geomorphological Research Group Technical Bulletin 28:* GeoBooks, Norwich, 107pp.

Thompson, S. M.; Adams, J. 1981: Suspended load in some major rivers of New Zealand. *In* Murray, D. L. and Ackroyd, P. (eds): *Physical Hydrology, New Zealand experience.* New Zealand Hydrological Society, Wellington: 213–29.

Yalin, M. S. 1972: *Mechanics of Sediment Transport.* Pergamon, Oxford 290 pp.

Yalin, M. S.; Karahan, E. 1979: Inception of sediment transport. *Journal of the Hydraulics Division, Proceedings of the American Society of Civil Engineers 105(11):* 1433–43.

Zeller, J. 1963: Einfuhrung in den Sedimenttransport offener Gerinne. *Schwiez. Bauzeitung Jgg 81.* (Referenced by Graf 1971: *op cit).*

Zingg, Th. 1935: Beitrag zur Schotteranalysen. *Schweizer Mineralog. Petrog Mitt. 15:* 39–140.

LIST OF SYMBOLS

		Units
d	particle diameter	m
d_i	particle diameter of surface material in the ith percentile	m
$d_{50,84,90}$	particle diameter with 50, 84, 90% finer	m
d_{50}'	median particle diameter of sub-surface material	m
d_{10x}	average diameter of the 10 largest clasts in a deposit	m
f	Darcy-Weisbach friction factor	-
g	acceleration due to gravity (9.81 ms^{-2})	ms^{-2}
h	flow depth	m
n	Manning's roughness coefficient	$m^{1/3}s^{-1}$
Q	flow discharge	m^3s^{-1}
q	flow discharge per unit width	m^2s^{-1}
Q_{10}	peak discharge of a 10-year recurrence interval flood	m^3s^{-1}
R	hydraulic radius	m
Rep	particle Reynolds number	-
S, S_e	channel bed, energy slopes	-
u	flow velocity	ms^{-1}
u^*	shear velocity	ms^{-1}
w	flow width	m
γ_f	unit weight of fluid	Nm^{-3}

γ_s	unit weight of sediment	Nm^{-3}
θ	dimensionless shear stress	-
θ'	dimensionless shear stress when Rep $>$ 100	-
τ_o	bed shear stress	Nm^{-2}
υ	kinematic viscosity	m^2s^{-1}